Human flavin-containing monooxygenase 3 on graphene oxide for drug metabolism screening

Human flavin-containing monooxygenase 3 on graphene oxide for drug metabolism screening

Silvia Castrignanò[1], Gianfranco Gilardi[1,2], Sheila J. Sadeghi[1,2]*

[1]Department of Life Sciences and Systems Biology, University of Torino, via Accademia Albertina 13, 10123 Torino, Italy.

[2]Centre for Nanostructured Interfaces and Surfaces, University of Torino, via Pietro Giuria 7, 10125 Torino, Italy.

AUTHOR INFORMATION

Corresponding Author

*Email: sheila.sadeghi@unito.it Tel.: +39-011-6704528. Fax: +39-011-6704643.

ABSTRACT: Human flavin-containing monooxygenase 3 (hFMO3) a membrane-bound hepatic protein, belonging to the second most important class of phase-1 drug metabolizing enzymes, was immobilized in its active form on graphene oxide (GO) for enhanced electrochemical response. In order to improve protein stabilization and to ensure the electrocatalytic activity of the immobilized enzyme, didodecyldimethylammonium bromide (DDAB) was used to mimic lipid layers of biological membranes and acted as an interface between GO nanomaterial and the hFMO3 biocomponent. GATR-FTIR experiments confirmed the preservation of the protein secondary structure and fold. Electrochemical characterization of the immobilized enzyme with GO and DDAB on glassy carbon electrodes was carried out by cyclic voltammetry where several parameters including redox potential, electron transfer rate and surface coverage were determined. This system's biotechnological application in drug screening was successfully demonstrated by the N-oxidation of two therapeutic drugs, benzydamine (nonsteroidal anti-inflammatory) and tamoxifen (anti-estrogenic widely used in breast cancer therapy and chemoprevention), by the immobilized enzyme.

Introduction

Among the five different functional human flavin-containing monooxygenases (hFMO) belonging to the mammalian FMO family, hFMO3 is described as the most important isoform present in the adult liver[1] having a prominent role in the metabolism of drugs and chemicals.[2] FMO enzymes are microsomal, flavin adenine dinucleotide containing, nicotinamide adenine dinucleotide phosphate-dependent[1-4] and are able to use molecular oxygen to catalyze the oxygenation of a variety of structurally different xenobiotics, including many therapeutic drugs.[5,6] All soft nucleophilic molecules possessing highly polarizable electron lone pairs on their heteroatoms are putative substrates for these enzymes.[1,3,6] hFMO3 catalyzes the selective oxygenation of the heteroatom by incorporation of one atom of molecular oxygen.[4,6] These reactions are usually considered to be part of the phase-1 drug metabolism detoxification process whereby compounds are transformed into highly polar and excretable molecules.[7] Unlike cytochromes P450, the hFMO3 activity produces few toxic metabolites and therefore could be used to control drug clearance with significant clinical advantage.[2] Therefore the design of drugs that are metabolized by hFMO3 rather than by cytochromes P450 is considered extremely advantageous.[2] Moreover, the hFMO3 is not readily induced or inhibited, like cytochromes P450, consequently minimising potential adverse drug-drug interactions.[8] Previously, we have described the engineering of a solubilised form of hFMO3 that has been characterised by direct electrochemistry in terms of its catalytic activity towards several drugs including benzydamine, sulindac sulfide, tamoxifen and aurora kinase inhibitors.[9-12]

In this work we developed a hFMO3 bio-electrode by immobilising hFMO3 protein in a nano-scaled system, based on graphene oxide (GO) in the presence of DDAB on glassy carbon electrodes.

Owing to its attractive properties, graphene has been used as a transducer to develop a number of different biosensing methodologies: bio-field-effect transistors, electrochemical biosensors, impedance biosensors, electrochemiluminescence, and fluorescence biosensors, as well as biomolecular labels.[13-15]

Among graphene derivatives, GO plays a major role in the development of carbon nanomaterials. GO can be produced by complete exfoliation of graphite oxide, obtaining a single graphene sheet widely functionalized.[16]Unlike graphene, whose structure is only composed by sp^2 hybridized carbon atoms, GO has a carbon structure that is interspersed by a range of oxygen-containing functional groups giving rise to some degree of sp^3 hybridization. Experimental data support the model proposed by Lerf and colleagues[17,18] in which the basal plane of the carbon sheet binds hydroxy- and epoxy-functional groups. Carbonyl groups are mainly present as carboxylic groups at the edge of the sheet.[19]

The abundance of oxygen functional groups are advantageous for GO electrochemical applications[20,21] and are expected to promote the electron-transfer between electrode substrates and enzyme molecules for the study of their direct electrochemistry.[22] Oxygen-containing groups also allow GO to be suspended in water and make it feasible for use in a variety of chemical reactions and compatible with biological applications not available to graphene, since it is insoluble in water and needs to be supported on a substrate.[23,24]

A key issue in the development of GO based bio-analytical systems is the stabilization of the bio-molecule together with the preservation of its native structure and activity. The latter becomes crucial when dealing with enzyme based electrochemical systems in which the catalytic activity is strongly dependent on the correct fold of the enzyme. In this regard, the use of a stabilizing component that could support both the preservation of enzymatic structure and activity, and the electrochemical interaction between the bio-component and the GO based transducer could be greatly advantageous.

To this end, surfactant films of synthetic lipid like didodecyldimethylammonium bromide (DDAB) provide a biomembrane-like microenvironment containing enough water for supporting structure and activity of proteins on electrode surfaces by acting as stable lyotropic liquid crystal coats.[25]

Here we report the development of a GO based nanostructured electrode system exploitable for the pharmacological screening of novel hFMO3 metabolized drugs by immobilizing this enzyme on GO modified glassy carbon in the presence of DDAB as a biomembrane-like surfactant. To our knowledge this is the first report of the use of GO with this class of human enzymes.

Experimental section

Chemicals. GO (4 mg/mL, water dispersion) was purchased from Graphenea (Spain). Analytical grade chemicals were used with no further purification. All solutions were prepared with ultra pure deionized water. DDAB, benzydamine (hydrochloride), benzydamine N-oxide (hydrogen maleate) and tamoxifen were purchased from Sigma-Aldrich, tamoxifen N-oxide was purchased from Biozol (Germany) and their solutions prepared immediately before use by dissolving the adequate amount in the appropriate solvent.

Expression and purification of wild type human FMO3. Wild type hFMO3 protein was expressed in *Escherichia coli* (JM109) and purified from the membrane fractions via nickel affinity chromatography, following the procedure described by Catucci and coworkers.[26] After the purification, the protein was visualized in a 10% SDS-polyacrylamide gel and stained with Coomassie Blue to verify its purity. The hFMO3 protein concentration was calculated assuming a molecular

mass of 56 kDa, a molar content equal to that of FAD and an extinction coefficient of 11,300 M^{-1} cm^{-1} at 450 nm.[27] The activity of the solubilized enzyme was measured by its N-oxidation of benzydamine where a K_M of 22 μM was measured which is similar to previously published values.[28]

Transmission electron microscopy. High resolution images of GO in the presence of DDAB were collected by TEM (JEOL-3010 UHR, Jeol Ltd., Japan, operating at 300 keV) at room temperature. Specimens for TEM observation were prepared by casting one drop of DDAB chloroform solution and of GO water dispersion onto an amorphous carbon film supported on a copper mesh grid and drying in air.

Fourier transform infrared spectroscopy. Infrared spectra of hFMO3, both in the presence and absence of GO, were acquired using the grazing angle attenuated total reflectance (GATR) tool. Human FMO3-DDAB samples were prepared on gold-PET flat surface substrates following the same procedure described for glassy carbon electrodes and compared with hFMO3 samples prepared by gently mixing equal volumes of hFMO3 solution and buffer (50 mM phosphate buffer pH 7.4 with 20% glycerol). Before the FT-IR analysis, samples were kept overnight at 4°C. All spectra were collected from 4000 to 800 cm^{-1} using a Bruker Model Tensor 27 FT-IR spectrometer (Bruker Instruments, Billerica, MA) with a scan velocity of 10 kHz and a resolution of 4 cm^{-1}. During data acquisition, the spectrometer was continuously purged with nitrogen at room temperature. Data were collected in triplicates and spectra were averaged using the Opus software (Bruker Instruments, Billerica, MA). Spectra of the protein were corrected by subtraction of the control samples acquired under the same scanning and temperature conditions. In particular, IR spectra of buffer, DDAB and DDAB-GO were used with the same dilution as background for hFMO3, hFMO3-DDAB and hFMO3-DDAB-GOsamples, respectively. Information on the number and location of components for the amide I band was provided by the Fourier self deconvolution conducted on the average spectra, using a deconvolution factor of 50 and a noise reduction factor of 0.8. Subsequently, curve fitting was performed using PeakFit software (SPSS Inc., USA).

Electrode preparation. Glassy carbon electrodes were modified with 10 μL of 20 mM DDAB chloroform solution or DDAB plus 5 μL of GO water dispersion and then left at room temperature for 10 minutes to allow solvent evaporation. 5 μL of purified hFMO3 solution (100 μM) or free FAD solution were added and the modified glassy carbon electrodes were kept at 4°C for 2 hours before any further experimental procedure.

Cyclic voltammetry and chronoamperometry. All electrochemical experiments were carried out at room temperature (25 °C) and in 50 mM phosphate buffer pH 7.4, containing 100 mM KCl as

supporting electrolyte, using an Autolab PGSTAT12 potentiostat (Ecochemie, The Netherlands) controlled by GPES3 software. A conventional three-electrode glass cell, equipped with a platinum wire counter electrode, an Ag/AgCl (3 M NaCl) reference electrode and 3 mm diameter glassy carbon working electrode (BASi, USA), was also used.

Electrochemical investigation of hFMO3 properties, both in the presence and in the absence of GO was performed by cyclic voltammetry in a nitrogen atmosphere within a glovebox (Belle Technologies, UK). Cyclic voltammograms were recorded between 0 and -750 mV at increasing scan rates.

Electrochemically driven substrate oxygenation by the hFMO3-DDAB-GO was performed using chronoamperometry with an applied potential bias of -650 mV for 15 min. In order to allow substrate permeation into the enzymatic layer and minimize mass transport influence at the transducer surface, hFMO3 was immobilized through DDAB-GO on glassy carbon rotating disk electrodes. All electrocatalysis experiments were performed using a BASi RDE-2 rotator system (BASi, USA) at 200 rpm rotation speed. Chronoamperometric procedure was applied on freshly prepared hFMO3-DDAB-GO electrodes in the presence of increasing concentrations of benzydamine or tamoxifen and the product(s) obtained after the 15 min reaction was immediately injected in HPLC for separation and quantification. Product quantification was achieved using calibration curves obtained, both for benzydamine N-oxide and for tamoxifen N-oxide, injecting standard solutions of known concentrations.

High performance liquid chromatography. The quantification of electrocatalysis product formed was performed by HPLC coupled with a diode array UV detector (Agilent-1200, Agilent technologies, USA) equipped with a 4.6 x 150 mm, 5 µm Eclipse XDB-C18 column, as previously reported.[11] Benzydamine and benzydamine N-oxide were separated using a linear gradient elution programmed as follows: linear gradient elution from 20% to 40% acetonitrile and from 80% to 60% 50 mM KH_2PO_4, 0-10 min; isocratic elution of 40% acetonitrile and 60% 50 mM KH_2PO_4, 10-12 min; linear gradient elution from 40% to 60% acetonitrile and from 60% to 40% 50 mM KH_2PO_4, 12 min-end of the run. The flow rate was set at 1 mL/min and detection wavelength was 308 nm. Retention times were 17.5 min and 20 min for benzydamine N-oxide and benzydamine, respectively. Tamoxifen and tamoxifen N-oxide were separated using an isocratic elution of 82% methanol and 18% triethylamine (1%), flow rate 0.8 mL/min. Detection wavelength was set at 278 nm. Retention times were 7 min and 15 min for tamoxifen N-oxide and tamoxifen, respectively.

Results and discussion

TEM images of GO in the presence of DDAB were collected in order to investigate the morphological features of GO layers distribution (Figure 1). As can be seen in the figure, GO is well distributed in a two dimensional manner as a foil-like material, with exfoliated sheets characterized by wrinkling and waviness, in agreement with previously published experimental data.[29-31] TEM results indicate that GO sheets are distributed throughout the electrode surface and that DDAB stabilized protein molecules should be able to directly interface with the GO layer.

The preservation of the hFMO3 3D fold in the presence of DDAB and GO was investigated by FTIR spectroscopy (Figure 2). As can be seen the collected spectra are effectively similar with amide I, II and III bands which are characteristics of protein IR spectra. Amide I band (~1650 cm^{-1}) is related to stretching vibration of peptidic carbonyl group with a minor contribution from the out-of-phase C-N stretching vibration.[32] This band results from the overlapping of a group of signals containing information on the secondary structure composition of the enzyme. Bands centred at around 1545 cm^{-1} can be assigned to the amide II band, which is due to the out-of-phase combination of the peptidic N-H in plane bend and the C-N stretching vibration. The peak at 1517 cm^{-1} is due to the C-C stretch and C-H bend of side chain tyrosine residues.[32] In addition, a set of bands can be observed in the region between 1200 and 1400 cm^{-1} that can be assigned to the amide III mode, associated to the in-phase combination of the peptidic N-H with C-N bending vibration.[32] In general the infrared spectral features of hFMO3 protein do not seem to be affected by the presence of GO with the enzyme structural integrity and fold preserved.

A deeper investigation of the secondary structure composition of hFMO3 protein was performed by fitting the amide I band with component bands after identification of their position through the deconvolution of the amide I peak (Figures 3A and 3B). Amide I component bands were then assigned to the corresponding protein secondary structure[32,33] and their contribution to the secondary structure composition of hFMO3 enzyme was calculated as percentages for the protein in the presence and in the absence of GO.

The secondary structure composition of hFMO3 is compared in Table 1 to the one measured in the presence of DDAB and DDAB-GO. As seen in the table, results obtained are highly comparable both in terms of peak positions and of percentage contributions. Moreover, these results are also in agreement with previously published data on the hFMO3 secondary structure calculation by far-UV circular dichroism and FTIR.[11,26]

Cyclic voltammetry of hFMO3 was carried out both on DDAB and on DDAB-GO glassy carbon electrodes. The cyclic voltammograms shown in Figure 4 demonstrate the electrochemical

reversibility of immobilized hFMO3 both in the presence and in the absence of GO. No voltammetric peaks were observed in the absence of the enzyme (data not shown). Redox peak potential values of hFMO3-DDAB and hFMO3-DDAB-GO electrodes are summarized and compared to those of free FAD in Table 2. Interestingly, it was found that the presence of GO shifts the redox potential, calculated as midpoint potential ($E_{1/2}$), towards more positive values both for hFMO3 bound and free FAD. As expected, the redox potential of the protein-bound FAD is shifted towards more negative values compared to free FAD, both in the presence and in the absence of GO. No significant differences were found when comparing peak-to-peak separation values due to GO. The presence of peak current values were found to be linearly dependent on the scan rate up to 120 mV (Figure 4, inset). As stated by Laviron's theory,[34] this property is characteristic of thin film confined electroactive species that are not under diffusion control. A significant increase of the redox peak current values was also observed due to the presence of GO ($P < 0.001$). Apparent surface coverage (Γ) of the electroactive hFMO3 bound and free FAD was calculated from the peak current plot versus scan rate by applying Faraday's law. Apparent surface coverage was increased by GO presence both in the case of protein bound and of free FAD. The observed increases were statistically significant (statistical analysis was performed by one-way ANOVA followed by Student-Newman-Keuls post hoc test).

The electron transfer rate constant (k_s) was also calculated from empirically fitted Laviron's equations.[34] To this end, irreversible electrochemistry of hFMO3 protein was studied in cyclic voltammetry by increasing the scan rate from 10 to 22 V s^{-1} and cathodic and anodic peak potentials were plotted versus the logarithm of the scan rate. The k_s values were calculated from the intercept of the E plot versus the natural logarithm of scan rate and were determined to be 38.6 ± 2.3 s^{-1} for hFMO3-DDAB and 48.1 ± 3.0 s^{-1} for hFMO3-DDAB-GO electrodes.

Direct electrochemical investigation of hFMO3 on DDAB-GO glassy carbon electrodes revealed an improvement of the electrochemical performance of the enzyme due to the presence of GO in terms of electron transfer rate. Moreover, GO increases the redox potential of both hFMO3 bound and free FAD confirming that FAD acquires a higher tendency to be reduced in DDAB-GO glassy carbon electrodes. This is highly advantageous for the electrocatalysis performance of hFMO3 protein since a protein which is more prone to reduction is likely more catalytically efficient. GO also enhances peak currents of hFMO3 enzyme, leading to an improvement of the signal-to-noise ratio. Moreover, a higher apparent surface coverage value was also observed for hFMO3-DDAB-GO electrodes, proving that in the presence of GO the amount of electroactive enzyme molecules on the electrode surface are increased.

Catalytic activity of hFMO3 on GO electrodes was examined using benzydamine and tamoxifen by chronoamperometry on glassy carbon rotating disk electrodes. Benzydamine is a nonsteroidal anti-inflammatory drug that is metabolized to its N-oxide by hFMO3.[35]

Benzydamine is a nonsteroidal anti-inflammatory drug that has been mainly used as a marker substrate of hFMO3 and its N-oxidation is usually referred to as an indicator of hFMO3 catalytic activity. Tamoxifen is an anti-estrogenic drug widely used in breast cancer therapy and chemoprevention that is also N-oxygenated by hFMO3 to its N-oxide.[36,37] The calculation of apparent kinetic parameters for the N-oxidation of these two drugs was performed by electrocatalysis followed by HPLC separation of the products. Reaction rate values were estimated after the quantification of the product formed during the electrocatalysis experiment and corrected by subtraction of the relevant controls (Figure 5A and B).

Control experiments were performed on DDAB-GO rotating disk electrodes using denatured hFMO3 protein (treated with 8 M guanidinium chloride for 30 min). Apparent Michaelis-Menten constant (K'_M) and turnover number (k'_{cat}) values were calculated for benzydamine and tamoxifen N-oxygenation by fitting velocity plot versus substrate concentration with Michaelis-Menten type curves. Calculated K'_M and k'_{cat} parameters for benzydamine electrocatalysis were 52.9 ± 6.4 μM and 62.3 ± 1.6 min^{-1}, respectively. Whereas for tamoxifen electrocatalysis K'_M and k'_{cat} values were estimated to be 5.8 ± 1.0 μM and 16.4 ± 0.6 min^{-1}, respectively.

Apparent kinetic values obtained for hFMO3 in the presence of GO were compared with previously published data for both benzydamine[11,26,28,38] and tamoxifen[36,37]and are reported in Table 3. Regarding benzydamine catalysis, our results are generally in good agreement with previously published data especially the calculated K'_M values (around 50-60 μM). For tamoxifen, our electrochemically determined K'_M value of 5.8 μM is much lower than the published values (121 and 1430 μM) which shows a better affinity. However, the calculated k'_{cat} value of 16.4 min^{-1} is lower than the only other reported value of 61 min^{-1}.[38] In this case, it was more difficult to compare our values with published results due to the limited availability of data regarding kinetics of hFMO3 turnover in the presence of tamoxifen, especially regarding recombinant systems. Furthermore, it must be taken into account that in our method reducing equivalents are provided by the electrode transducer and not NADPH, and that the enzyme velocity is directly measured by estimating product formation whereas the only available data about hFMO3 turnover in the presence of tamoxifen is based on the NADPH consumption assay (which provides an indirect measurement of enzyme catalysis).

When comparing benzydamine electrocatalysis results for hFMO3 in the presence of GO with our previously published data about hFMO3 electrocatalysis, a significant improvement of the enzyme catalytic efficiency, expressed as apparent turnover number, was observed.

Finally, the reproducibility of the results obtained from different electrodes expressed as residual standard deviation, was calculated to be 15%.

Conclusions

The biocompatibility of inorganic nanomaterials is a crucial issue for the successful development of protein based high throughput electrochemical assay systems. Due to its interesting electrochemical and mechanical properties, GO can be considered as an attractive nanomaterial and has been used as a high performance electrochemical transducer to develop a number of bioanalytical paradigms. However, enzyme stabilization is essential in order to optimize electrocatalytic performance and electrochemical tuning between the nanostructured transducer and the protein biocomponent.

In this work, the unique features of GO have been applied to hFMO3 electrochemical properties using the stabilizing capability of the synthetic lipid DDAB to develop a sensitive, high performing bioelectrochemical assay for the screening of drugs metabolized by hFMO3. The direct electrochemical response of hFMO3 was enhanced by the presence of GO in terms of electron transfer rate, current signal-to-noise ratio and apparent surface coverage. Moreover, catalytic efficiency of the enzyme in the presence of GO, determined by the kinetic parameters K'_M and k'_{cat} for benzydamine and tamoxifen were found to be comparable with previously published data. Both FTIR and electrochemical characterization of hFMO3-DDAB-GO glassy carbon electrodes were found to be consistent with the preservation of the protein structure and fold. Moreover, compared to our previously obtained electrocatalysis results, GO improves the electrocatalytic efficiency of hFMO3 enzyme.

The use of GO in the presence of DDAB can be considered as a novel clinically relevant biotechnological approach with potential application in not only high throughput screening of new chemical entities as possible drugs metabolized by hFMO3, but also deciphering the implications of hFMO3 polymorphism in drug metabolism, i.e. Personalized Medicine.

Author Contributions

The manuscript was written through contributions of all authors. All authors have given approval to the final version of the manuscript.

Notes

The authors declare no competing financial interest.

ACKNOWLEDGMENT

The authors wish to acknowledge financial support from the Progetto Ateneo-San Paolo 2012.

Supporting Information Available

This information is available free of charge via the Internet at http://pubs.acs.org/.

REFERENCES

(1) Cashman, J. R. *Drug Discov Today* **2004**, 9, 574-581.

(2) Cashman, J. R. *Expert Opin. Drug. Metab. Toxicol.* **2008**, 4, 1507-1521.

(3) Cashman, J. R. *Chem. Res. Toxicol.* **1995**, 8, 166-181.

(4) Krueger, S. K.; Williams, D. E. *Pharmacol. Ther.* **2005**, 106, 357-387.

(5) Phillips, I. R.; Dolphin, C. T.; Clair, P.; Hadley, M.R.; Hutt, A. J.; McCombie, R. R.; Smith, R. L.; Shephard, E. A. *Chem. Biol. Interact.* **1995**, 96, 17-32.

(6) Cashman, J. R. *Drug Metab. Rev.* **2002**, 34, 513-521.

(7) Cashman, J. R. *Curr. Drug. Metab.* **2000**, 1, 181-191.

(8) Cashman, J. R. *Biochem. Biophys. Res. Commun.* **2005**, 338, 599-604.

(9) Sadeghi, S. J.; Meirinhos, R.; Catucci, G.; Dodhia, V. R.; Di Nardo, G.; Gilardi, G. *J. Am. Chem. Soc.* **2010**, 132, 458-459.

(10) Castrignanò, S.; Sadeghi, S. J.; Gilardi, G. *Anal. Bioanal. Chem.* **2010**, 398, 1403-1409.

(11) Castrignanò, S.; Sadeghi, S. J.; Gilardi G. *Biochim. Biophys. Acta.* **2012**, 1820, 2072-2078.

(12) Catucci, G.; Occhipinti, A.; Maffei, M.; Gilardi, G.; Sadeghi, S. J. *Int. J. Mol. Sci.* **2013**, 14, 2707-2716.

(13) Pumera, M. *Mater. Today* **2011**, 14, 308-315.

(14) Artiles, M. S ; Rout, C. S.; Fisher, T. S. *Adv. Drug. Deliv. Rev.* **2011**, 63, 1352-1360.

(15) Kuila, T.; Bose, S.; Khanra, P.; Mishra, A. K.; Kim, N. H.; Lee, J. H. *Biosens. Bioelectron.* **2011**, 26, 4637-4648.

(16) He, H. Y.; Riedl, T.; Lerf, A.; Klinowski, J. *J. Phys. Chem.* **1996**, 100, 19954-19958.

(17) Lerf, A.; He, H.; Forster, M.; Klinowski, J. *J. Phys. Chem. B* **1998**, 102, 4477–4482.

(18) He, H. Y.; Klinowski, J.; Forster, M.; Lerf, A. *Chem. Phys. Lett.* **1998**, 287, 53–56.

(19) Compton, O. C.; Nguyen, S. T. *Small* **2010**, 6, 711-723.

(20) McCreery, R. L. *Chem. Rev.* **2008**, 108, 2646-2687.

(21) Shan, C.; Yang, H.; Song, J.; Han, D.; Ivaska, A.; Niu, L. *Anal. Chem.* **2009**, 81, 2378-2382.

(22) Banks, C. E.; Davies, T. J.; Wildgoose, G. G.; Compton, R. G. *Chem. Commun. (Camb)* **2005**, 7, 829-841.

(23) Galande, C.; Gao, W.; Mathkar, A.; Dattelbaum, A. M.; Narayanan, T. N.; Mohite, A. D.; Ajayan, P. M. *Part. Part. Syst. Charact.* **2014**, 31, 619-638.

(24) Dreyer, D. R.; Todd, A. D.; Bielawski, C. W. *Chem. Soc. Rev.* **2014**, 43, 5288-5301.

(25) Rusling, J. F. *Acc. Chem. Res.* **1998**, 31, 363-369.

(26) Catucci, G.; Gilardi, G.; Jeuken, L.; Sadeghi, S. *J. Biochem. Pharmacol.* **2012**, 83, 551-558.

(27) Macheroux, P. in *Flavoprotein Protocols: Methods in Molecular Biology*; Chapman, S.K., Reid, G.A., Eds; Humana Press: Totowa, 1999; pp. 1-7.

(28) Lang, D. H.; Rettie, A. E. *Br. J. Clin. Pharmacol.* **2000**, 50, 311-314.

(29) Zhou, M.; Zhai, Y.; Dong, S. *Anal. Chem.* **2009**, 81, 5603-5613.

(30) Dikin, D. A.; Stankovich, S.; Zimney, E. J.; Piner, R. D.; Dommett, G. H.; Evmenenko, G.; Nguyen, S. T.; Ruoff, R.S. *Nature* **2007**, 448, 457-460.

(31) Wang, K.; Ruan, J.; Song, H.; Zhang, J.; Wo, Y.; Guo, S.; Cui, D. *Nanoscale Res. Lett.* **2011**, 6, 8-15.

(32) Barth, A.; Zscherp, C. Q. *Rev. Biophys.* **2002**, 35, 369-430.

(33) Barth, A. *Biochim. Biophys. Acta* **2007**, 1767, 1073-1101.

(34) Laviron, E. *J. Electroanal. Chem.* **1979**, 101, 19-28.

(35) Hamman, M. A.; Haehner-Daniels, B. D.; Wrighton, S. A.; Rettie, A. E.; Hall, S. D. *Biochem. Pharmacol.* **2000**, 60, 7-17.

(36) Hodgson, E.; Rose, R. L.; Cao, Y.; Dehal, S. S.; Kupfer, D. J. Biochem. *Mol. Toxicol.* **2000**, 14, 118-120.

(37) Krueger, S. K.; Vandyke, J. E.; Williams, D. E.; Hines, R. N. *Drug Metab. Rev.* **2006**, 38, 139-147.

(38) Shimizu, M.; Yano, H.; Nagashima, S.; Murayama, N.; Zhang, J.; Cashman, J. R.; Yamazaki, H. *Drug Metab. Dispos.* **2007**, 35, 328-330.

Table 1. Calculated secondary structure content of immobilized hFMO3 from the deconvolution of the Amide I band of FTIR spectra.

Structure	hFMO3		hFMO3-DDAB		hFMO3-DDAB-GO	
	Peak Position	Area	Peak position	Area	Peak position	Area
α helix	1658 cm^{-1} 1666 cm^{-1}	34.9 %	1658 cm^{-1} 1668 cm^{-1}	36.7 %	1657 cm^{-1} 1666 cm^{-1}	34.5 %
β sheet	1630 cm^{-1}	20.9 %	1629 cm^{-1}	20.2 %	1629 cm^{-1}	20.7 %
Turn	1674 cm^{-1} 1685 cm^{-1}	21.5 %	1677 cm^{-1} 1688 cm^{-1}	20.4 %	1676 cm^{-1} 1688 cm^{-1}	23.6 %
Unordered	1648 cm^{-1}	22.7 %	1647 cm^{-1}	22.7 %	1647 cm^{-1}	21.3 %

Fit quality (R^2) between original and fitted spectra ≥ 0.99.

Table 2. Redox properties of hFMO3 in the presence and absence of GO compared to those of free FAD.

	$E_{1/2}$ / mV	ΔE / mV	Γ / pmol cm^{-2}
GC/hFMO3-DDAB	-363.2 ± 1.0	61.0 ± 1.7	19.5 ± 2.7
GC/hFMO3-DDAB-GO	-354.7 ± 0.3 $^{(*)}$	64.0 ± 1.0	32.1 ± 1.9 $^{(**)}$
GC/FAD-DDAB	-353.7 ± 3.5 $^{(\#)}$	50.7 ± 9.6 $^{(\#)}$	27.6 ± 0.2 $^{(\#)}$
GC/FAD-DDAB-GO	-344.3± 4.0 $^{(*,\#)}$	49.3 ± 1.5 $^{(\#)}$	64.9±6.9 $^{(***,\#\#)}$

(*) $P < 0.05$, (**) $P < 0.01$, (***) $P < 0.001$ when comparing data obtained in the absence of GO. ($^{\#}$) $P < 0.05$, ($^{\#\#}$) $P < 0.001$ when comparing data obtained with hFMO3 protein.

363 **Table 3. Comparison of apparent kinetic parameters for benzydamine and tamoxifen N-oxidation with previously**
364 **published results.**

	Expression system	Enzymatic activity assay	K_M (μM)	k_{cat} (min^{-1})	
Benzydamine	*E. coli*	Electrode immobilization	58.9 ± 9.1	63.2 ± 2.2	Present work
	E. coli	Electrode immobilization	52.1 ± 9.5	0.47 ± 0.02	Castrignanò et al., 2012
	E. coli	Solution	56 ± 8	9 ± 2	Catucci et al., 2012
	E. coli	Solution	51 ± 19	300 ± 27	Shimizu et al., 2007
	Baculovirus	Solution	80 ± 8	36 ± 2	Lang and Rettie, 2000
Tamoxifen	*E. coli*	Electrode immobilization	5.8 ± 1.1	16.4 ± 0.6	Present work
	Baculovirus	NADPH consumption	121 ± 25	61 ± 20	Krueger et al., 2006
	E. coli	NADPH consumption	1430	n.d.	Hodgson et al., 2000

365

366

FIGURE CAPTIONS

Figure 1. TEM images of GO in the presence of DDAB taken from four different regions of the modified grid.

Figure 2. FTIR spectra of DDAB stabilized hFMO3 protein in the absence and presence of GO compared to that of only hFMO3 protein solution.

Figure 3. Amide I band with individual components fitted for hFMO3 in the absence (A) and in the presence (B) of GO.

Figure 4. Anaerobic cyclic voltammograms of hFMO3 on DDAB glassy carbon electrodes in the absence (dashed line) and in the presence (solid line) of GO. Scan rate: 120 mV s^{-1}. Inset: plot of cathodic (filled symbols) and anodic (empty symbols) peak currents versus scan rate for hFMO3 on DDAB glassy carbon electrodes in the absence (triangles) and in the presence (circles) of GO. $R^2 >$ 0.99.

Figure 5. Bioelectrocatalytically produced benzydamine N-oxide (A) and tamoxifen N-oxide (B) by hFMO3-GO-DDAB glassy carbon electrodes: plot of reaction velocity versus substrate concentration fitted to the Michaelis-Menten equation. Data are shown as mean ± SD of three different electrode measurements.

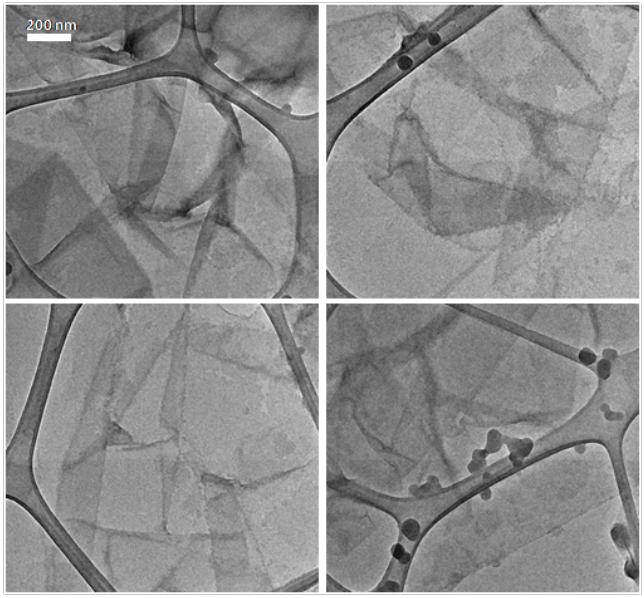

Figure 1

391

392

393

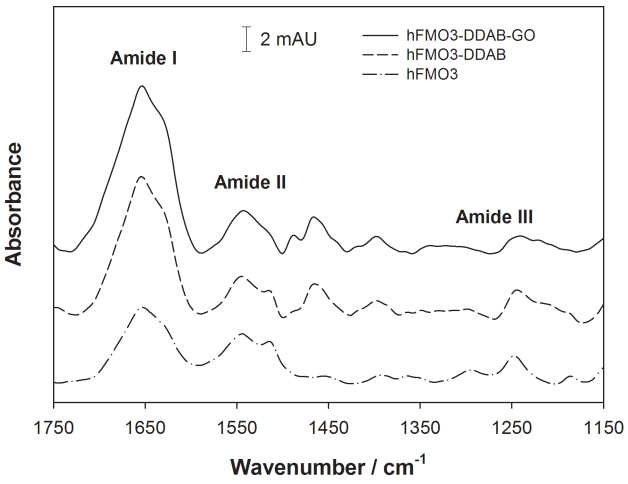

394

395

396 Figure 2

397

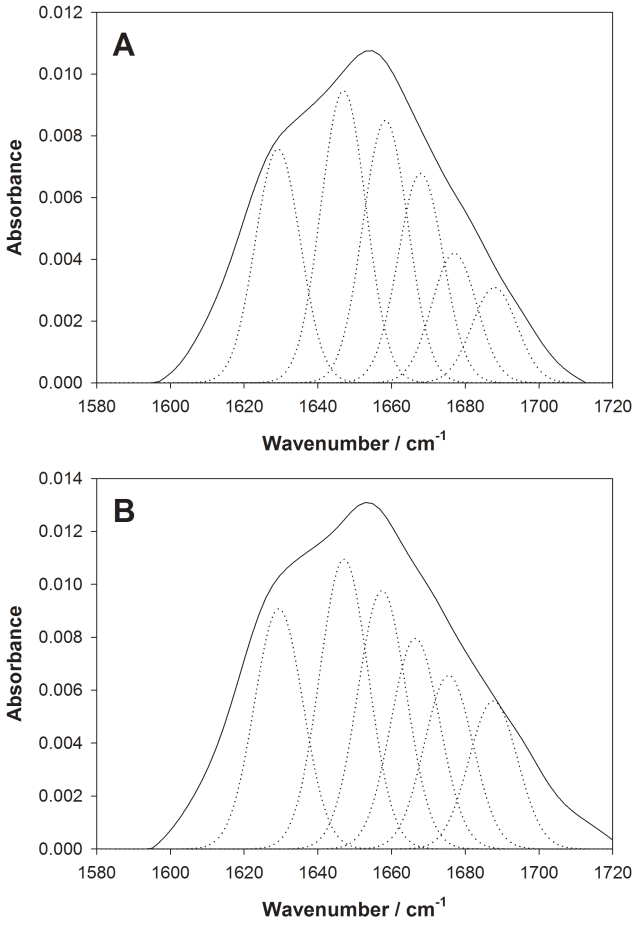
A
B
Absorbance
Wavenumber / cm-1
0.000
0.002
0.004
0.006
0.008
0.010
0.012
0.014
1580
1600
1620
1640
1660
1680
1700
1720

Figure 3

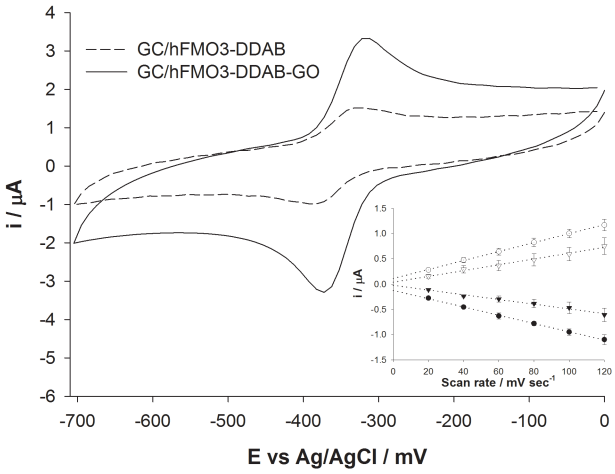
GC/hFMO3-DDAB
GC/hFMO3-DDAB-GO
i / µA
E vs Ag/AgCl / mV
Scan rate / mV sec-1

Figure 4

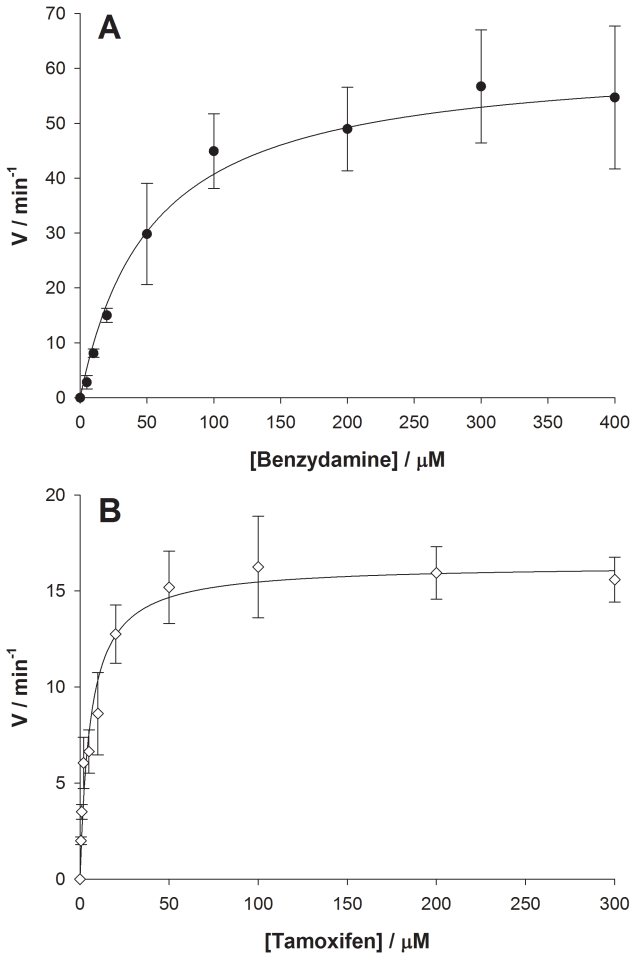

Figure 5

For TOC only

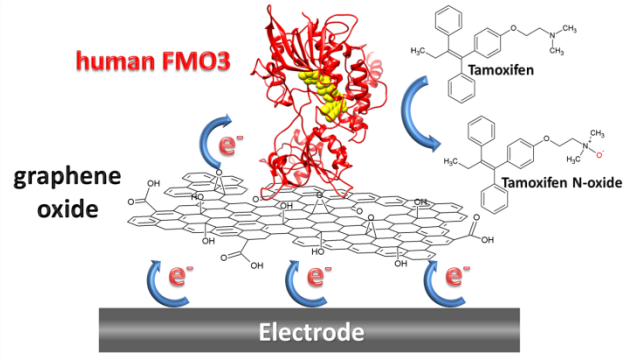
human FMO3
Tamoxifen
Tamoxifen N-oxide
graphene
oxide
e⁻
e⁻
e⁻
e⁻
Electrode